

Atomic nature of reconstructed Si(110)

H. Neddermeyer and St. Tosch

Institut für Experimentalphysik der Ruhr-Universität Bochum, D-4630 Bochum, Federal Republic of Germany

(Received 4 May 1988)

Using scanning tunneling microscopy (STM) we have measured constant-current topographies of reconstructed Si(110). While low-energy-electron diffraction (LEED) showed a 4×5 pattern with dominant 2×1 contributions, in STM a 2×5 periodicity of atomic building blocks is observed. These building blocks are arranged in the form of chains along $[\bar{1}10]$ -like directions and show a tendency to pairing, which accounts for the 4×5 LEED results. The 2×1 reconstruction, which was previously ascribed to a high-temperature phase of Si(110), is explained by a reduction of chain length caused by the generation of defects with increasing temperature.

On Si(110) a large number of ordered surface structures have been observed. In the first low-energy-electron diffraction (LEED) study of this surface Jona found in addition to an initial structure a 4×5 , 2×1 , 5×1 , and $7(9)\times 1$ reconstruction.¹ An interesting aspect of this surface was later reported by Olshanetsky and Shklyayev, who interpreted some of these reconstructions in terms of order-order phase transitions, which according to their results occur with increasing temperature.² In particular, on heating of a 4×5 reconstructed surface a 2×1 LEED pattern was observed above 600°C , which changed to 5×1 at a temperature of 750°C . In more recent investigations³⁻⁶ most of the known reconstructions were associated with the presence of a small Ni contamination of the surface, while clean Si(110) should only exhibit a " 16×2 "⁴ or a " 32×2 "⁴ periodicity.⁷ According to Ref. 4 the sensitivity of Si(110) against Ni-induced reconstructions should be similar as for Si(111), which in this case develops a $\sqrt{19}\times\sqrt{19}R23.4^\circ$ structure.⁸

By using scanning tunneling microscopy (STM) we have studied surfaces of Si(110), which are prepared by *short* (typically 1 min) high-temperature annealing in order to avoid roughening and facetting, which is usually observed on Si surfaces after extended heating cycles.⁹ The samples show a distinct 4×5 LEED pattern with particular high intensity of the half and integral order beams (corresponding to a 2×1 reconstruction), whereas the STM images are characterized by chainlike arrangements of structures along $[\bar{1}10]$ with 2×5 unit cells. The orientation of the unit cells mostly agrees in adjacent chains and therefore accounts for the 4×5 LEED pattern. On the other hand, many defects are found on this surface leading to large variations of the chain length (typically between a few and many tens of unit cell dimensions), which explains the high intensity of the 2×1 beams. The 4×5 -to- 2×1 order-order phase transition² is reinterpreted by a loss of order along $[\bar{1}10]$ with increasing temperature. Contamination of the surfaces with Ni is ruled out in our experiment.

The present results have been obtained by means of reverse-view LEED optics and a scanning tunneling microscope described in detail elsewhere.^{10,11} As substrates, we used *p*-type (B-doped, $6\ \Omega\text{cm}$) Si(110) wafers. They are clamped on a Ta sample holder by means of Ta strips.

Prior to mounting in the microscope they were chemically cleaned in acetone and rinsed in methanol and deionized water. *In situ* treatment consisted in degassing and one or two heating cycles at approximately 1100°C for 1 min in a vacuum of better than 10^{-10} mbar. A small cooling rate was chosen ($\approx 2^\circ\text{C/s}$) in order to obtain a room-temperature equilibrium surface structure. The LEED pattern showed the presence of a 4×5 reconstruction and was similar to that reported by Olshanetsky and Shlyayev.² However, the half and integral order beams were particularly strong. The STM images were obtained in the form of constant-current topographies (CCT's) and are displayed in the form of gray-tone images. Both polarities of the sample bias voltage have been utilized. Ordered and reconstructed areas have been obtained on large parts of the surface (typically $100\times 100\ \text{nm}^2$). We note that the same sample preparation in case of Si(111) generated large areas with 7×7 reconstruction with no indication of a Ni-induced $\sqrt{19}\times\sqrt{19}R23.4^\circ$ structure.

CCT's are displayed in top view for negative (Fig. 1) and positive sample bias (Fig. 2). Except for subtraction of an oblique plane no drift correction or smoothing procedure has been applied to the data, which covers approxi-

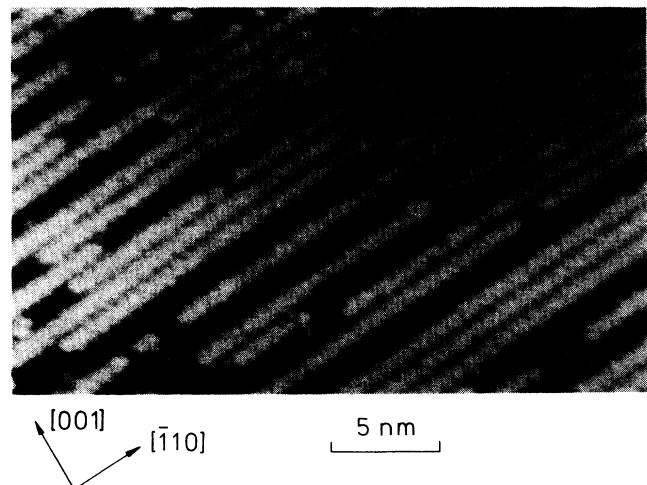


FIG. 1. CCT (top view) from Si(110) obtained at a sample bias $U = -2\ \text{V}$ and a tunneling current $I = 2\ \text{nA}$. The area is $\approx 14\times 30\ \text{nm}^2$.

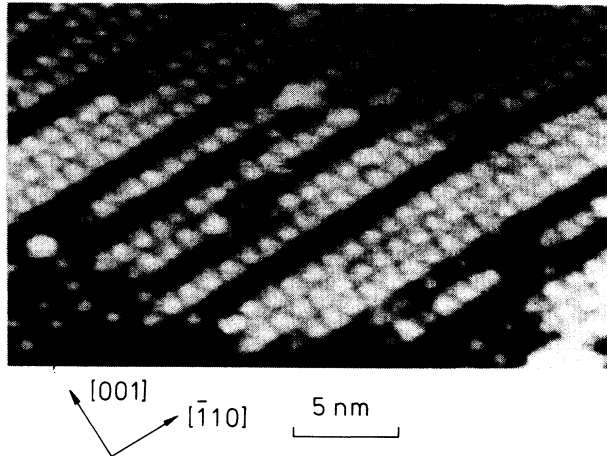


FIG. 2. CCT (top view) from Si(110) obtained at $U=2$ V and $I=2$ nA. The area is $\approx 15 \times 24$ nm².

mately the same part of the surface. Large-area scans show the presence of monoatomic and double-atomic steps in an average distance of 10–20 nm, which do not follow a well-defined crystallographic direction. The reconstruction appears as a chainlike structure in the $[\bar{1}10]$ direction. The surface is not fully covered by these chains. They are interrupted in a random way leading to a statistically varying length. In some cases, the chains are missing. The corrugation across the troughs was determined to 0.14–0.20 nm, which is in good agreement with an expected value of 0.19 nm or a missing atomic layer of Si(110). The atomic structure of the reconstruction appears in form of neighboring V's with alternating direction. In the case of tunneling from occupied states of the sample these V's do not show much height variations (Fig. 1), while for tunneling into unoccupied states these V's carry a protruding feature on the apex. These protruding parts form a kind of zigzag structure along $[\bar{1}10]$. A statistical analysis of the orientation of these V's shows that they are arranged preferentially by doubling the periodicity of the surface normal to the chains.

For derivation of an atomic model of the reconstruction, the STM measurements have been repeated with smaller x and y increments during scanning [Fig. 3(a)]. The positions of the observed structures are schematically plotted in Fig. 3(b). The V's consist of the already mentioned protrusion (visible in Fig. 2) and two somewhat lower protrusions as indicated in Fig. 3(b) by large and small dots, respectively. The raster of the unit cells is included for better orientation. A paired arrangement of chains is seen [2 and 3, of Fig. 3(b)] as well as a depression of the same width [4 of Fig. 3(b)] showing no reconstruction and two chains with a phase slip of opposite direction [1 and 6 of Fig. 3(b)]. Using the known sensitivity of the xy piezoelectric system the dimension of the unit cell was determined to 1.17×1.98 nm², which is in good agreement with the expected size of 1.09×1.92 nm² for a 2×5 reconstruction of Si(110).

For comparison with the ideal Si(110) surface the average position of the observed structures has been determined from the CCT shown in Fig. 3. The results are col-

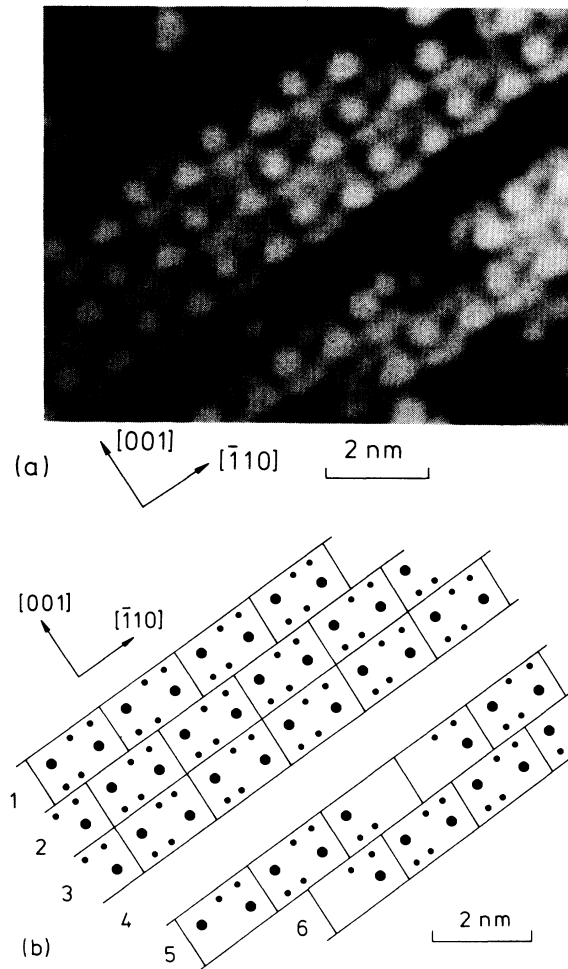


FIG. 3. (a) CCT (top view) from Si(110) obtained at $U=1$ V and $I=2$ nA. (b) Schematic representation of (a), which has been obtained from a top view CCT with a slightly different size and which included lines of constant height for more precise data evaluation.

lected in Fig. 4(a) in a coordinate system in units of the lattice parameter of the surface (0.384 nm). The position of the protrusions located on the coordinate axes have been fitted to the ideal lattice by a linear change of the scale and a drift correction in order to obtain the correct angle between $[001]$ and $[\bar{1}10]$. The position of the remaining features are given in the same coordinate system. It is evident that the observed protrusions are located on less symmetrical positions than expected. For example, the zigzag structure of the protrusions visible already in Fig. 2 is not generated by an equidistant arrangement of atomic features. The shape of the above mentioned V's is also not consistent with the existence of a simple mirror plane containing the $[001]$ direction. Another observation is that differences of locations cannot be described in terms of integral numbers of the lattice parameter, which consequently excludes high-symmetry positions on the ideal lattice.

In Fig. 4(b), we show an arrangement of the observed features for both polarities of the sample bias voltage on top of ideally terminated Si(110), which we have chosen

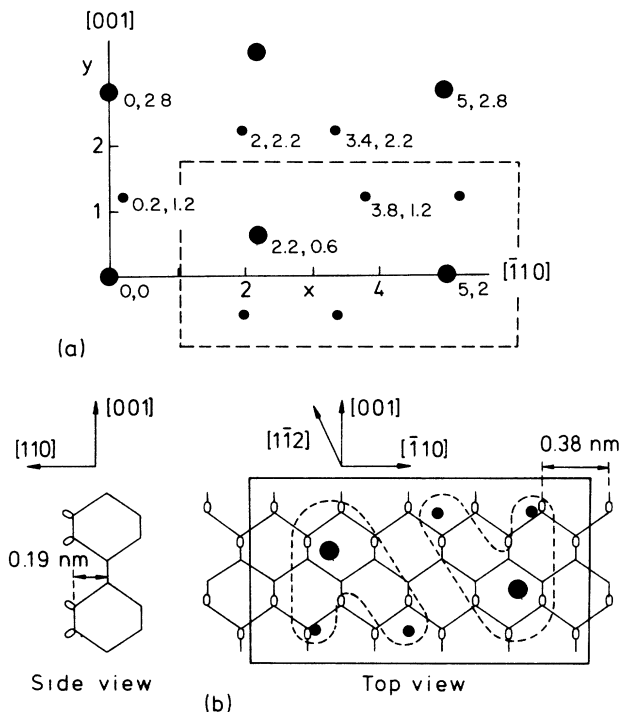


FIG. 4. (a) Numerical values for position of structures of CCT shown in Fig. 3. (b) The same structures plotted on ideal Si(110), where the dangling bonds are symbolized by open ovals.

on the basis of various arguments. Ideal Si(110) is characterized by zigzag chains of atoms carrying one dangling bond each. The size of the 2×5 unit cell requires the participation of two such chains in the surface reconstruction. Since the unreconstructed troughs have the same width as that of the chains (see Figs. 1 and 2), we conclude that the 2×5 unit cells contain two complete zigzag chains of dangling bonds of the ideal lattice along [001] as shown in Fig. 4(b). In this case, the deeper-lying trough contains one complete zigzag chain of dangling bonds, which would not be the case for a different arrangement of the 2×5 surface mesh in the [001] direction. For alignment of the unit cell along $[\bar{1}10]$ we argue that the higher protrusions are most likely located on a kind of adatom position, where three dangling bonds of the second atomic layer are saturated by a Si adatom. Due to the nonintegral distances (in terms of the lattice parameter) this is only possible in an approximate way, but a different arrangement than chosen in the figure would place these features even more asymmetric on the Si lattice. The position of the lower protrusions (positive sample bias) is then automatically found on the edges of the ideal dangling bond chains. However, their orientation along $[\bar{1}10]$ cannot be explained by a simple model of binding to the second atomic layer.

An interesting difference is seen for the atomic structures obtained at a positive sample bias [dots in Fig. 4(b)] corresponding to tunneling into empty states of the sample and for those measured with negative sample bias [dashed

lines in Fig. 4(b)] corresponding to tunneling into the filled states of Si(110). We note that the latter data do not show many details even when measuring in a more dense raster scan than has been employed in Fig. 1. While both polarities lead to the same gross shape of the V-like atomic structures, characteristic differences are seen on a more close inspection of the CCT's. The regions between large and small dots in one V appear as depression when looking on the unoccupied states, which is filled in case of tunneling from occupied states. The opposite behavior is recognized for the regions between the small dots within each V. This observation is certainly related to the formation of bonding and antibonding states in the atomic subunits, which are visibly more pronounced for negative and positive sample bias, respectively.

The derivation of an atomic model for reconstructed Si(110) seems to be very difficult, since only appreciable distortions in (at least) the second atomic layer allow a satisfactory explanation of the structure seen with STM. It is obvious that a simple dimerization of atoms from neighboring zigzag chains of the ideal lattice¹² cannot account for the observed complicated atomic pattern. Such a dimerization should ideally be visible in form of wormlike structures with little corrugation in the $[\bar{1}10]$ direction, probably similar to STM results on Si(100) 2×1 (Ref. 9) or GaAs(110).¹³ Since we have never observed such structures we have some doubt whether the transition from a 4×5 to a 2×1 LEED pattern may be explained by an order-order phase transition.² We suggest that a reduction of the number of subunits in the reconstructed chains may well account for the disappearance of the 4×5 LEED pattern.

Some comments should be made on the nature of the other reconstructions known for Si(110). They can roughly be divided into two groups, those which are described by the periodicity of the ideal lattice along $[\bar{1}10]$ (i.e., 5×1 , 7×1 , and 9×1) and those which show a rotated pattern (i.e., " 16×2 " and " 32×2 "). As a matter of fact, the large number of atomic defects visible in our results already indicates that the ordering principle is more local than in case of, e.g., the 7×7 reconstruction of Si(111). This implies that on the introduction of extrinsic defects as steps or impurities, which may develop in particular after prolonged preparation cycles of the sample, the macroscopic surface may change drastically. Since we used each of our samples only in one STM experiment with a corresponding short heating time we believe that our observed CCT's are representative for the initial reconstruction of Si(110). We note that at the steps visible in some of our images (except for a necessary phase slip parallel to the step direction) no particular influence on the observed reconstruction was found. Ishikawa, Hosokawa, Hamaguchi, and Ichinokawa have observed the growth of domain boundaries of the " 16 " structure parallel to $[\bar{1}12]$ steps,¹³ which is not confirmed by our results. A different and in particular longer lasting procedure may be responsible for the occurrence of such reconstructions, which, on the other hand, are more difficult to study with STM because of increasing roughness.

In summary, we have obtained atomically resolved STM images from reconstructed Si(110), which has

developed a 4×5 LEED pattern. The unit cells consist of two atomic building blocks, which have the shape of V's and are arranged in a 2×5 periodicity of the ideal surface. They preferentially form pairs of chains, which account for the 4×5 LEED pattern. The high-temperature 2×1 structure is explained by a reduction of the chain length with increasing temperature. The position of the atomic

features indicates that at least the second atomic layer is severely distorted compared to the ideal structure.

This work has been supported by the Deutsche Forschungsgemeinschaft. We thank G. Hackel for continuous technical support and Wacker-Chemitronic (Burghausen) who provided us with the Si wafers.

¹F. Jona, IBM J. Res. Dev. **9**, 375 (1965); see also H. D. Hagstrum and G. E. Becker, Phys. Rev. B **8**, 1580 (1973).

²B. Z. Olshanetsky and A. A. Shlyaev, Surf. Sci. **67**, 581 (1977); see also B. A. Nesterenko, A. V. Brovii, and A. I. Sorokovykh, *ibid.* **171**, 495 (1986).

³T. Ichinokawa, H. Ampo, S. Miura, and A. Tamura, Phys. Rev. B **31**, 5183 (1985).

⁴H. Ampo, S. Miura, K. Kato, Y. Ohkawa, and A. Tamura, Phys. Rev. B **34**, 2329 (1986).

⁵Y. Yamamoto, S. Ino, and T. Ichikawa, Jpn. J. Appl. Phys. **25**, L331 (1986).

⁶S. Miura, K. Kato, T. Ide, and T. Ichinokawa, Surf. Sci. **191**, 259 (1987).

⁷Values have been given in parentheses since the refraction pattern is generated by a rotated structure.

⁸R. J. Wilson and S. Chiang, Phys. Rev. Lett. **58**, 2575 (1987); previous work on Ni/Si(111) is cited therein.

⁹R. J. Hamers, R. M. Tromp, and J. E. Demuth, Phys. Rev. B **34**, 5343 (1986).

¹⁰Th. Berghaus, A. Brodde, H. Neddermeyer, and St. Tosch, Surf. Sci. **184**, 273 (1987).

¹¹Th. Berghaus, A. Brodde, H. Neddermeyer, and St. Tosch, Surf. Sci. **193**, 235 (1988).

¹²W. A. Harrison, Surf. Sci. **55**, 1 (1976).

¹³Y. Ishikawa, Y. Hosokawa, I. Hamaguchi, and T. Ichinokawa, Surf. Sci. **187**, L606 (1987).

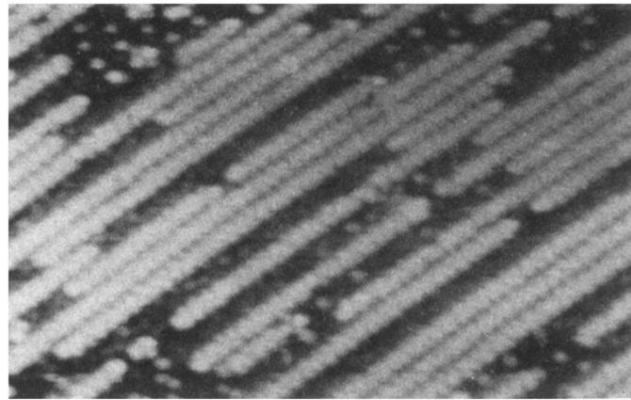


FIG. 1. CCT (top view) from Si(110) obtained at a sample bias $U = -2$ V and a tunneling current $I = 2$ nA. The area is $\approx 14 \times 30$ nm².

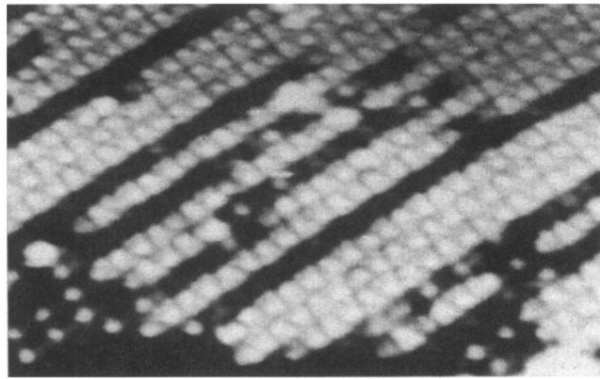


FIG. 2. CCT (top view) from Si(110) obtained at $U=2$ V and $I=2$ nA. The area is $\approx 15 \times 24$ nm².

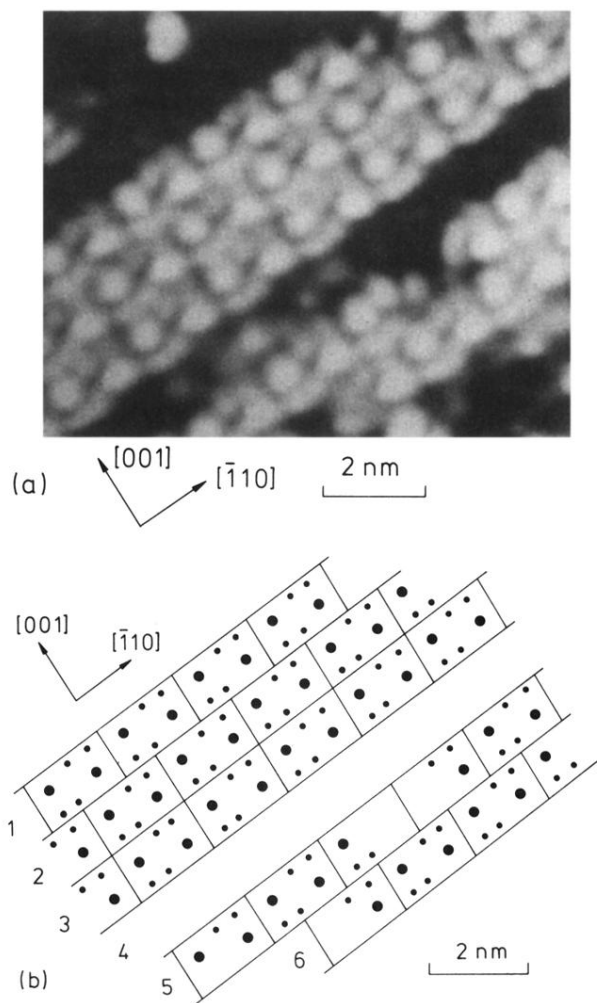


FIG. 3. (a) CCT (top view) from Si(110) obtained at $U = 1$ V and $I = 2$ nA. (b) Schematic representation of (a), which has been obtained from a top view CCT with a slightly different size and which included lines of constant height for more precise data evaluation.